Chapter 2
Fundamentals of Biosensors and Application of MALDI-ToF-MS in Bio-diagnostic Domain

Abstract In this chapter, fundamentals of biosensor devices are explained with a special emphasis on optical biosensors such as enzyme-linked immunosorbent assay (ELISA). Current chapter introduces a novel polymeric material that can be used as a substitution of poly methyl methacrylate (PMMA), which is one of the mostly applied materials in fabrication of ELISA well plates. Proposed polymeric material is a copolymer synthesized in free-radical polymerization reaction with methyl methacrylate (MMA) and methacrylic acid (MAA) as monomers. Potential analytical platforms made from this copolymer can overcome some of the major drawbacks of the conventional platforms made from PMMA. In order to have a close control over the chemical and physical properties of the developed material, this copolymer was synthesized in different compositions by variation of the monomers concentrations in polymerization reaction. All different composition of this copolymer has been thoroughly analyzed by MALDI-ToF-MS and results are discussed in a great detail. MADLI has been used as a powerful technique to provide essential information regarding structural formation of the polymer chains in each composition as well as end-groups analysis of the respective chains. Present chapter connects analytical data obtained from MALDI analysis with the application of these platforms as bioreceptor surfaces for antibody immobilization and subsequent virus detection. Developed platforms have been investigated by MALDI in respect to their chemical and physical properties and their suitability for their application in virus detection. Current chapter also explains that a carful design of the macromolecule is possible by controlling the reaction parameters. In that path, MALDI analysis plays a vital role in confirmation of the reaction's outcome. This chapter is dedicated to the MALDI analysis of a linear polymer chains with 2 monomers involved in synthesis reaction.

Keywords ELISA · Free-radical polymerization reaction · Protein immobilization · Hydrophilicity · Surface functional groups · Virus detection · Linear polymer chains

S. Hosseini and S.O. Martinez-Chapa, *Fundamentals of MALDI-ToF-MS Analysis*,
SpringerBriefs in Forensic and Medical Bioinformatics,
DOI 10.1007/978-981-10-2356-9_2

2.1 Biosensors

Biological sensors, or in the short form biosensors, are analytical systems capable of detecting biological entities from different categories. Biosensors have rapidly found variety of applications in many areas such as food quality control, medical diagnostics and environmental monitoring [1–4]. Basic principles in operation of biosensors rely on the translation of a biological response to an electrical signal by the help of a transducer [4]. Figure 2.1 presents the schematic presentation of a biosensor. The surface of the bioreceptor initially receives the analyte of interest (antibodies in the present case, Fig. 2.1). Bioreceptors are generally engineered in such a way that can accommodate approaching biomolecules on their surfaces.

Once antibodies are immobilized on the surface, they can readily couple with the respective antigens. Depending on the type of the assay, different protocols can be used in conducting an assay. But one thing is similar in all these different protocols [4]. Immediately after antigens and conjugated antibodies are coupled, a biological response is generated and sent to the transducers. This signal can further be amplified and displayed by the detector as a biorecognition result (Fig. 2.1). Transduction of the signal can be done via different approaches such as electrochemical biosensors, optical biosensors, cyclic voltammetry, electrochemical impedance spectroscopy, surface plasmon resonance (SPR), potentiometric signal transduction, gravimetric, and thermal transduction [4–8].

From the category of optical biosensors, enzyme-linked immunosorbent assay (ELISA) is one of the commonly applied immunoassays in conventional clinical practice. ELISA has variety of applications in different areas. As a plate-based assay, ELISA is mostly utilized for quantification of the biomolecules such as peptides, proteins, antibodies, viruses and hormones [9–12]. The detection approach follows the same strategy as shown in Fig. 2.1. Bioreceptor, in this case, is ELISA well plate, which is normally made of plastic materials and is available in different forms. The detector, in this technique, is an ELISA reader that records and translates the signal received from the well plate.

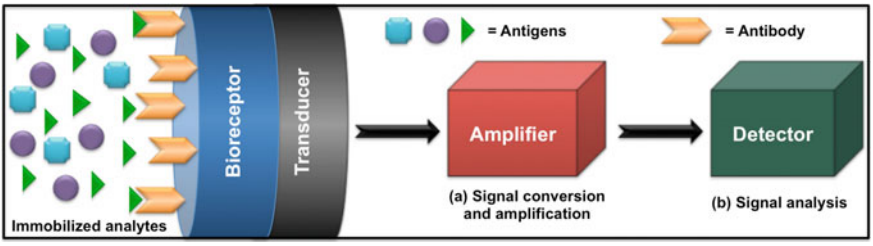

Fig. 2.1 Schematic representation of a biosensor: antibodies are immobilized on the surface of the bioreceptor and coupled with the specific antigens. Following this coupling, the analytical response was transferred from transducer to amplifier where this signal is enhanced and sent to the detector. Detector in the final step translates the signals which indicates the positivity or negativity of the infection

Although well-known ELISA assay has offered number of benefits such as cost effectiveness, safety and versatility of the assay, it is disadvantaged for its lengthy and labor-intensive procedure with relative inconsistency of the results [9, 10]. Maybe one of the main drawbacks of ELISA is the weak performance of the well plate itself. Polystyrene (PS) and/or poly methyl methacrylate (PMMA) are typical substrates used in fabrication of such analytical platforms. PS and PMMA offer unique properties such as cost-effectiveness, low specific weight, high impact resistance and flexibility [4]. But both polymers are relatively inert in their nature and lack surface functional groups that can promote bimolecular interaction [10, 13–20]. Presence of active functionalities such as amine ($–NH_2$), carboxyl (–COOH) or sulfhydryl (–SH) groups could enhance the plates' performance and lead to an effective analyte-surface interaction through physical and/or covalent immobilization [4, 10, 18, 21, 22].

In this chapter, new types of copolymer compositions are introduced. Synthetic compounds, in this study, are used to fabricate biochips that can be used in ELISA assay for enhanced detection of the viruses. Developed materials can also be used as the potential substrates for fabrication of a new generation of ELISA well plates with better performance than the conventional well plates. The newly developed copolymers contain pendant –COOH groups that can subsequently enhance their performance in detection of the viruses.

2.2 Synthesis of Poly Methyl Methacrylate-Co-Methacrylic Acid P(MMA-Co-MAA) and Preparation of the Biochips

Two monomers, methyl methacrylate (MMA) and methacrylic acid (MAA), have been chosen for the free-radical polymerization of poly methyl methacrylate-co-methacrylic acid P(MMA-co-MAA). The detailed polymerization procedure can be found in our previous publications [18, 19, 23]. The result of the polymerization with MMA as the sole monomer of the reaction would be PMMA, which is one of the major materials of choice for manufacturing ELISA well plates. Additional monomer (MAA) reforms this polymer into a new compound, which is a copolymer. While, P(MMA-co-MAA) possess almost most of the properties of PMMA, two polymeric materials have a minor difference that is the presence of –COOH groups derived from the MAA segments of the copolymer (Fig. 2.2).

It is expected that presence of –COOH groups impacts the performance of the copolymer material in virus detection as such functionalities are reactive towards $–NH_2$ groups of the proteins that exist in the structure of antibodies and/or antigens. Following this approach, it is anticipated that functional groups are evenly distributed inside the structure of the copolymers as well as the surface. In the case of hard plastic materials such as PMMA and/or P(MMA-co-MAA), the outmost layer of the surface is the interface zone where the analyte-surface interaction occurs.

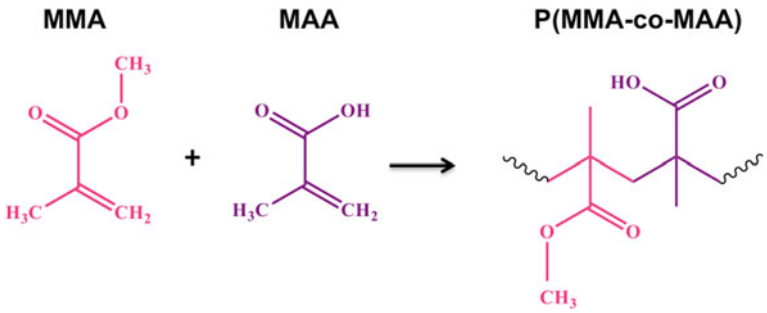

Fig. 2.2 Formation of P(MMA-co-MAA) from MMA and MAA as monomers

Therefore, surface engineering is of a crucial importance in the area of biomolecular interactions. Although existence of the reactive functional groups such as –COOH can be a good asset for a bioreceptor platform, only optimum number of such functionalities can be helpful for successful protein immobilization and consequent detection [17, 24]. In order to have a range of functionality distribution on the surface, different compositions of P(MMA-co-MAA) have been polymerized as shown in Table 2.1. Along with these different copolymer compositions, pure PMMA has also been polymerized to be used as a control. The variation in initial molar ratios of the monomers is the key factor in free-radical polymerization as tuning the monomer's concentration results in optimum –COOH distribution on the biosensor platforms [10, 17, 20, 25].

Synthesized copolymer compositions have been processed into the biochips by coating silicon wafers as substrate by the aim of spin-coating technique. Step by step of the coating process were explained in our previously published works [18, 19, 23, 26]. In brief, silicon wafers were thoroughly washed before coating and placed inside the spin-coating instrument (Laurell, model WS-650MZ-23NPP). With the speed of 3000 rpm, surface of the silicon wafer was coated with 5 % polymer solution for 55 s [18, 19, 26]. Finely coated biochip is shown in Fig. 2.3a, while Fig. 2.3b displays the cross-section image of the representative biochip. Cross-section view of the chips demonstrates the silicon wafer (substrate), P(MMA-co-MAA) layer (polymer coating) and the gold coated layer on the top of the polymer [27]. Gold or platinum coatings are normally required for SEM imaging of the polymers to avoid surface charging and to obtain high quality images [17–19, 26]. Coated silicon wafers were cut into the suitable size in order to fit into the ELISA well plate for further protein immobilization and virus detection (Fig. 2.3c).

Table 2.1 Initial molar ratios of the monomers involved in polymerization of P(MMA-co-MAA)

Compositions	MMA	MAA
PMMA	10	0
P(MMA-co-MAA) (9:1)	9	1
P(MMA-co-MAA) (7:3)	7	3
P(MMA-co-MAA) (5:5)	5	5

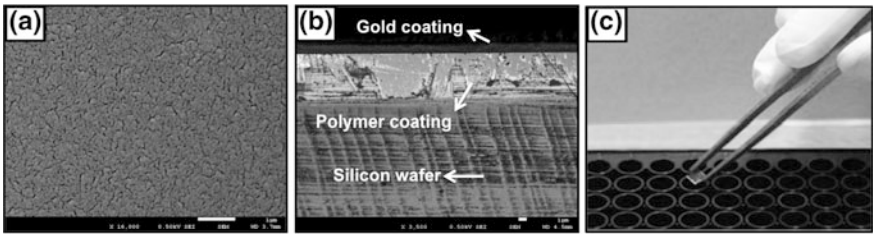

Fig. 2.3 SEM images from the frontal view (**a**), and cross-section of the representative biochips (**b**) as well as the digital photograph of a biochip (**c**)

2.3 Sample Preparation for MALDI Analysis

The MALDI-ToF-MS spectra of P(MMA-co-MAA) copolymer compositions were obtained after optimization of the procedure. This optimization process involved several different methods of sample preparation including mostly applied conventional methods. Nonetheless, it was observed that the layer-by-layer sample preparation technique provided the best quality of spectra [28]. For that reason this method was chosen as the preferred method for conducting MALDI experiments in all the chapters of this book.

By dissolving 10 mg of the polymers in 1 ml of tetrahydrofuran (THF), polymer solution was prepared for MALDI analysis. For matrix preparation, 100 mg of the selected matrix (2,5-Dihydroxybenzoic acid, DHB) was also dissolved in 1 ml of ethanol (EtOH). Ionizing agent was prepared by adding 100 mg of sodium iodide (NaI) in 10 ml of EtOH as well. Following the layer-by-layer sample deposition, matrix solution was initially deposited on the MALDI plate following by ionizing agent after first layer was dried. Subsequently, a polymer layer was spotted on the top of the crystallized DHB–NaI. After drying in ambient temperature, MALDI plate was placed in the MALDI-ToF-MS instrument (ABI 4800 plus) equipped with nitrogen laser (375 nm). The detector was operated in the positive ion reflection mode [18, 20].

2.4 MALDI Data Interpretation

2.4.1 Different Species as the Possible Products of Soft Ionization

Over the last decade, MALDI-ToF-MS has successfully become one of the leading techniques for investigation of both biological and synthetic polymers [29, 30]. Specifically, end-group analysis and accurate calculation of units distribution along with the structural analysis of the polymer chains were know as the advantageous

features of MALDI analysis [31, 32]. MALDI offers the soft ionization that differentiates this technique from other methods of mass spectrometry. As the final product, one or more of the following species are expected to be formed in soft ionization:

$[Poly. + H]^+$ (added proton)
$[Poly. - H]^-$ (removed proton)
$[Poly. + nH]^{n+}$ (more than 1 added protons)
$[Poly. + Na]^+$ (added sodium ion)
$[Poly. + nNa]^+$ (more than 1 added sodium ions).

2.4.2 General Structure of P(MMA-Co-MAA)

The structure of P(MMA-co-MAA) product in free-radical polymerization is shown in Fig. 2.4. Instead of X and Y in the position of end-groups, H or CH_3 can be replaced (Fig. 2.2). The letters outside the brackets (n and m) refer to the respective numbers for MMA and MAA monomers involved in polymerization reaction. The structure shown is Fig. 2.4 is a general form for all the possible products of the free-radical reaction in this study. For instant, in the case of pure PMMA, X and Y are both CH_3 groups while m = 0 and n can be 1, 2, 3, 4 or more.

2.4.3 MALDI Analysis of PMMA

MALDI spectrum presented in Fig. 2.5 sets the simplest example for structural calculations, in which the sole monomer is MMA and the product of the synthesis is expectedly PMMA. Herein, we present a step-by-step calculation of the polymer structure and molecular weight for the peak at m/z = 2031 (as an example) and the detailed explanation to show how this number (2031) can fit into the general structure shown in Fig. 2.4. As it can be predicted, end-groups (X and Y) are both CH_3 groups. In order to find a matching structure for this peak, the Mw of the MMA monomer (shown in pink color in Fig. 2.4) has to be initially determined.

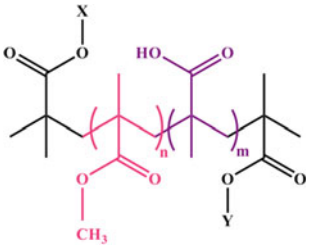

Fig. 2.4 General structure of P(MMA-co-MAA)

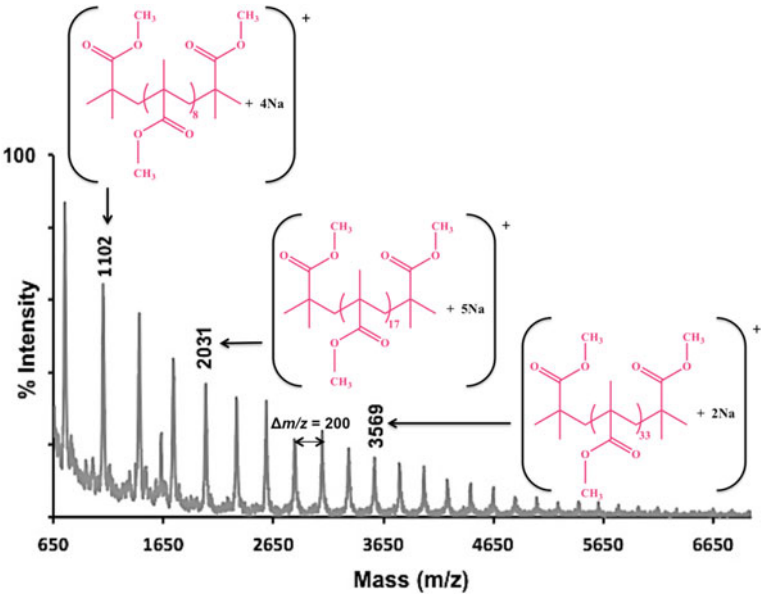

Fig. 2.5 MALDI spectrum of PMMA (reproduces with the permission from Hosseini et al. [20])

MMA segment in Fig. 2.4 contains 5 carbon (C) atoms, 2 oxygen (O) atoms as well as 8 hydrogen (H) atoms. Therefore, the Mw for this unit can be calculated as follows:

$$(5 \times 12) + (2 \times 16) + (8 \times 1) = 100 \quad (\text{Mw for MMA unit inside the chain})$$

The fact that each building unit of PMMA has the mass of 100 explains the intervals of $\Delta m/z = 200$ shown in Fig. 2.5. This number corresponds to the orderly increment of the MMA monomers in the structure of the polymer chains. In the other word, each chain/peak has 2 additional MMA units in its structure than the previous one.

Returning back to the peak at 2031, the special chain that is matched with this number can be clearly identified. As it was described, mass of MMA segment inside the chain is equal to 100. However, the same unit does not have the same mass when it located at the end-groups position. As it can be seen from any of the structures in Fig. 2.5, MMA unit as end-group (on the left side of the chain) consists of 6 atoms of C, 2 atoms of O and 11 atoms of H. Thus, the mass for this end-group can be calculated as follows:

$$(6 \times 12) + (2 \times 16) + (11 \times 1) = 115 \quad (\text{Mw for MMA unit as end-group})$$

MMA unit as the end-group on the right side of the chain, however, has 5 atoms of C, 2 atoms of O and 9 atoms of H and the total mass of this groups is:

$$(5 \times 12) + (2 \times 16) + (9 \times 1) = 101 \quad (\text{Mw for MMA unit as end-group})$$

To simplify the calculation, we can identify these three MMA species as:

$$\begin{aligned} &\text{MMA}_{\text{mass}} = 100 \quad (\text{repetitive unit inside the chain}) \\ &{}^{*}\text{MMA}_{\text{mass}} = 115 \quad (\text{star end-group}) \\ &{}^{**}\text{MMA}_{\text{mass}} = 101 \quad (\text{double star end-group}) \end{aligned}$$

Now, it can be seen that the peak at *m/z* = 2031 (Fig. 2.5) corresponds to:

$${}^{*}\text{MMA} + (\text{MMA} \times 17) + {}^{**}\text{MMA} + 5\text{Na} = 115 + 1700 + 101 + (5 \times 23) = 2031$$

It can be sometimes the case that the theoretical numbers do not match the exact experimental values resulted from MALDI analysis. For instance, in Fig. 2.5, proposed structure for the peak at *m/z* = 3569 corresponds to the mass of 3562. Nevertheless, this structure was found as the closest one to the mentioned peak value. It should be noted that minor differences in the theoretical and experimental values are negligible as molecules might have more than one additional proton attached to the chain in some special cases (presented species in Sect. 2.4.1). It also can be due to the fact that NaI, as the ionizing agent, might react with the polymer chain by rejecting one of the H atoms from the structure. In such cases, Na becomes part of the structure of the chain instead of an additional ion attached to the chain. Therefore, corresponding mass value for Na should be considered 22 not 23. Regardless of such minor alterations in mass values, chain structures can be identified in a relatively accurate fashion.

2.4.4 MALDI Analysis of P(MMA-Co-MAA)

MALDI analysis was performed on P(MMA-co-MAA) of different compositions and results are presented in Figs. 2.6, 2.7 and 2.8. Following the same strategy, different mass values for MAA units can be calculated as follows:

$$\begin{aligned} &\text{MAA}_{\text{mass}} = 86 \quad (\text{repetitive unit inside the chain}) \\ &{}^{*}\text{MAA}_{\text{mass}} = 101 \quad (\text{star end-group}) \\ &{}^{**}\text{MAA}_{\text{mass}} = 87 \quad (\text{double star end-group}) \end{aligned}$$

Figure 2.6 depicts the MALDI spectrum for analyzed P(MMA-co-MAA) (9:1) samples. Proposed structure for the peak located at *m/z* = 978 that perfectly

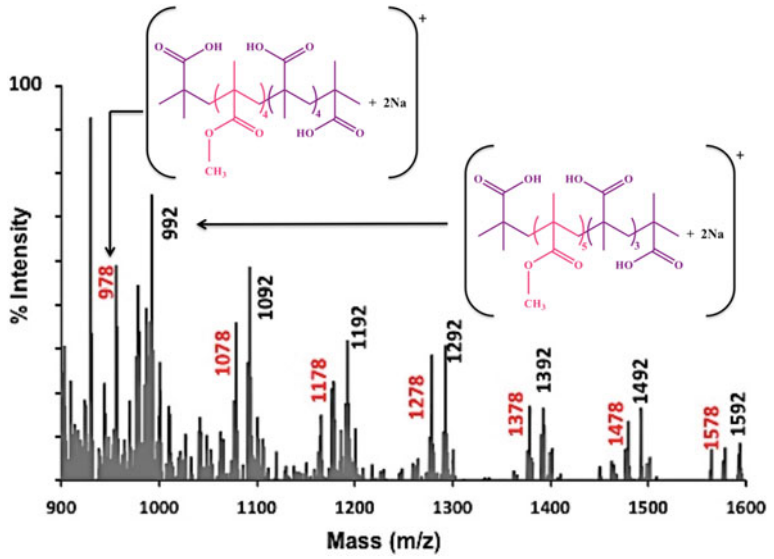

Fig. 2.6 MALDI spectrum of P(MMA-co-MAA) (9:1) (reproduces with the permission from Hosseini et al. [20])

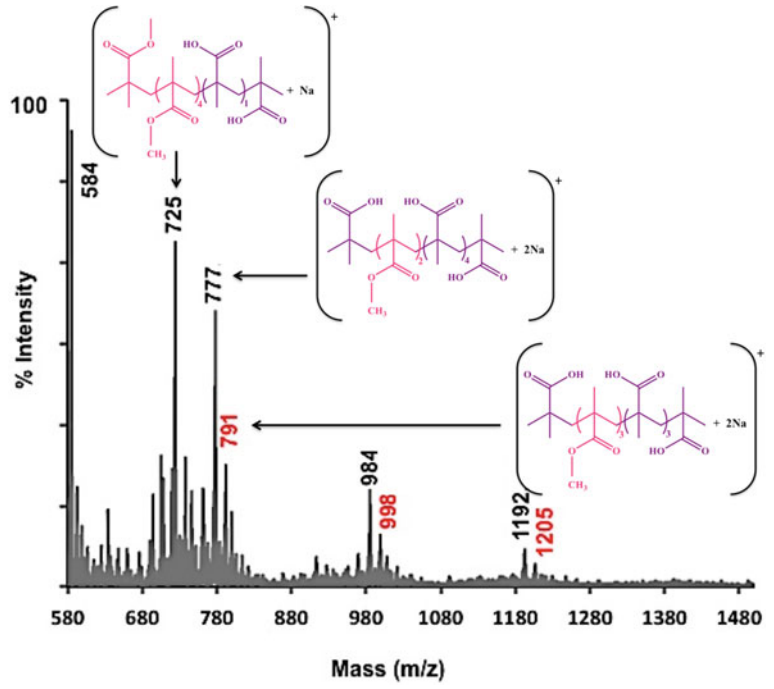

Fig. 2.7 MALDI spectrum of P(MMA-co-MAA) (7:3) (reproduces with the permission from Hosseini et al. [20])

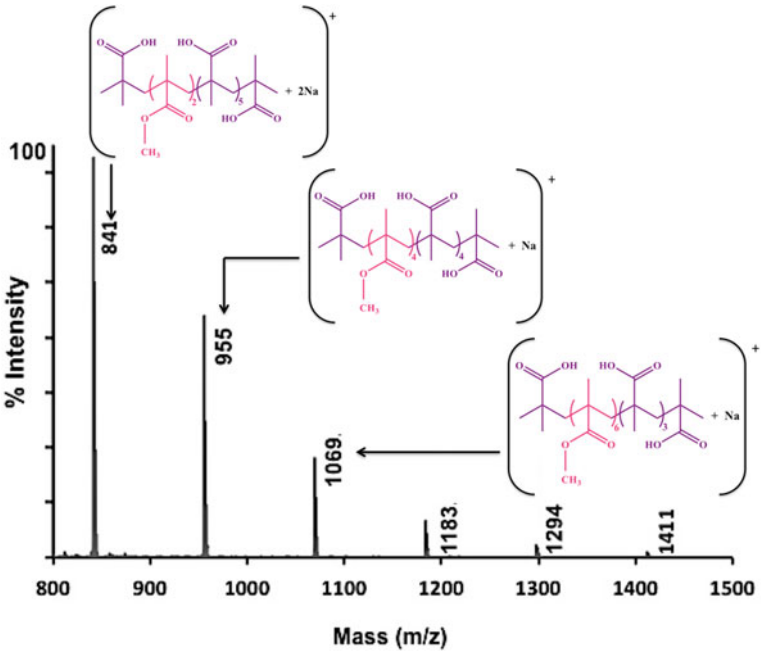

Fig. 2.8 MALDI spectrum of P(MMA-co-MAA) (5:5) (reproduces with the permission from Hosseini et al. [20])

matches the experimental value resulted from MALDI analysis is shown in Fig. 2.6. As it can be seen this structure corresponds to:

$$^{*}\text{MAA} + (\text{MMA} \times 4) + (\text{MAA} \times 4) + {}^{**}\text{MAA} + 2\text{Na} = 101 + 400 + 344 + 87 + 46 = 978$$

Proposed structure for peak at *m/z* = 992 consists of 5 units of each monomer (MMA and MAA), from which 2 of the 5 MAA monomers are located at the position of end-groups in this chain (Fig. 2.6).

Spectrum in Fig. 2.7 belongs to MALDI analysis of P(MMA-co-MAA) (7:3). As it can be observed from the spectrum, number of MAA units in assigned structures generally increased. This gradual increase in the number of MAA segments is a direct function of initial molar ratios of the monomers applied in free-radical polymerization reaction. For reminder, in the formation of P (MMA-co-MAA) (7:3), 30 % of the involved monomers in free-radical polymerization reaction were MAA, while only 10 % of the monomer reactants in polymerization of P(MMA-co-MAA) (9:1) were chosen to be MAA monomers.

Therefore, an overall increase in the number of MAA units in MALDI spectrum of composition (7:3) in comparison to that of composition (9:1) is expected.

The same trend can also be observed in the spectrum of analyzed P(MMA-co-MAA) (5:5), which is presented in Fig. 2.8. As the number of MAA segment in copolymer compositions increases, logically, the concentration of –COOH functional groups also increases. This increase in the number of surface functional groups happens not just inside the structure of the compound but also on the outmost layers of the composition. Therefore, it can be predicted that coated biochips with P(MMA-co-MAA) (5:5) have more –COOH functionalities on the surface in comparison to coated biochips with P(MMA-co-MAA) (7:3) or P(MMA-co-MAA) (9:1) copolymers. The availability of such functionality on the surface plays a vital role in analyte-surface interaction and subsequent virus detection, as it will be explained further in the text.

2.4.5 End-Group Analysis

MALDI analysis is a powerful technique in many different perspectives. Perhaps, one of the most valuable information that can be extracted from this analytical technique is the end-group analysis of the copolymer chains [20, 33]. Determination of the end-groups is of a great importance as such functionalities contribute in both, physical and chemical properties of the material [33]. In particular, when chemical modification of the material is aimed, end-group analysis offers essential information. Presence or absence of such terminal groups lead to the significant changes, not just in the characteristics of the polymer, but also in reactivity of the compound towards other species [34]. Table 2.2 provides detailed information regarding the number of monomers in each chain, end-groups as well as the experimental and theoretical mass values for each detected peak. X and Y in the general structure of the copolymer (shown in Fig. 2.4) can be replaced by "H" and/or "CH_3" depending on the individual chains. The gradual increase in the molar ratio of the MAA monomers can be clearly observed from Table 2.2, which is in agreement with pre-determined concentrations of monomers (MMA/MAA) in the polymerization reaction.

Although end-groups data obtained from MALDI analysis are essential, in some rare cases, it can result in the wrong understanding of the polymer chain. For example, in MALDI spectrum of P(MMA-co-MAA) (5:5), there is a peak with the *m/z* value of 1069. Detailed investigation of this particular peak leads to four different structures with completely different end-groups as Fig. 2.9 presents.

This special peak reveals different possible formations for a same polymer chain. Each of the proposed structures, in turn, can fit perfectly in the peak value (1069). In all of the suggested structures shown in Fig. 2.9, number of the monomers is constant (MMA = 6 and MAA = 5). Nevertheless, each structure suggests different terminal groups for its chain. Such exceptional cases prove that end-group study performed by MALDI can sometimes lead to the misinterpretation of the exact

Table 2.2 End-group identification from MALDI spectra analyzed for different composition of P(MMA-co-MAA)

Peak position (m/z)		MMA units (n)	MAA units (m)	X	Y
Exp.	*Theor.*	*PMMA*			
1102.160	1108	8	0	CH_3	CH_3
2036.91	2037	17	0	CH_3	CH_3
3569.40	3562	33	0	CH_3	CH_3
Exp.	*Theor.*	*P(MMA-co-MAA) (9:1)*			
992.519	992	5	3	H	H
1078.567	1078	5	4	H	H
1092.571	1092	6	3	H	H
1178.625	1178	6	4	H	H
1192.571	1192	7	3	H	H
1278.771	1278	7	4	H	H
1292.646	1292	8	3	H	H
1378.771	1378	8	4	H	H
1392.717	1392	9	3	H	H
1478.776	1478	9	4	H	H
1492.783	1492	10	3	H	H
1578.808	1578	10	4	H	H
1592.828	1592	11	3	H	H
Exp.	*Theor.*	*P(MMA-co-MAA) (7:3)*			
584.999	585	1	1	CH_3	CH_3
724.009	725	4	1	CH_3	H
777.936	778	2	4	H	H
791.94	792	3	3	H	H
984.889	984	3	4	CH_3	H
998.911	999	1	8	H	H
1192.911	1192	5	5	CH_3	CH_3
1205.869	1206	6	4	CH_3	CH_3
Exp.	*Theor.*	*P(MMA-co-MAA) (5:5)*			
841.570	841	2	5	H	H
955.658	995	4	4	H	H
1069.754	1069	6	3	H	H
1183.811	1183	1	8	H	H
1294.818	1294	1	11	H	CH_3
1411.949	1412	1	12	H	CH_3

Reproduces with the permission from Hosseini et al. [20]

macromolecular structures [20]. Therefore, it is highly recommended to take the advantage of MALDI analysis in association with other useful techniques such as nuclear magnetic resonance (NMR), X-ray photoelectron spectrometry (XPS), Fourier transform infrared (FTIR) spectroscopy and RAMAN spectroscopy.

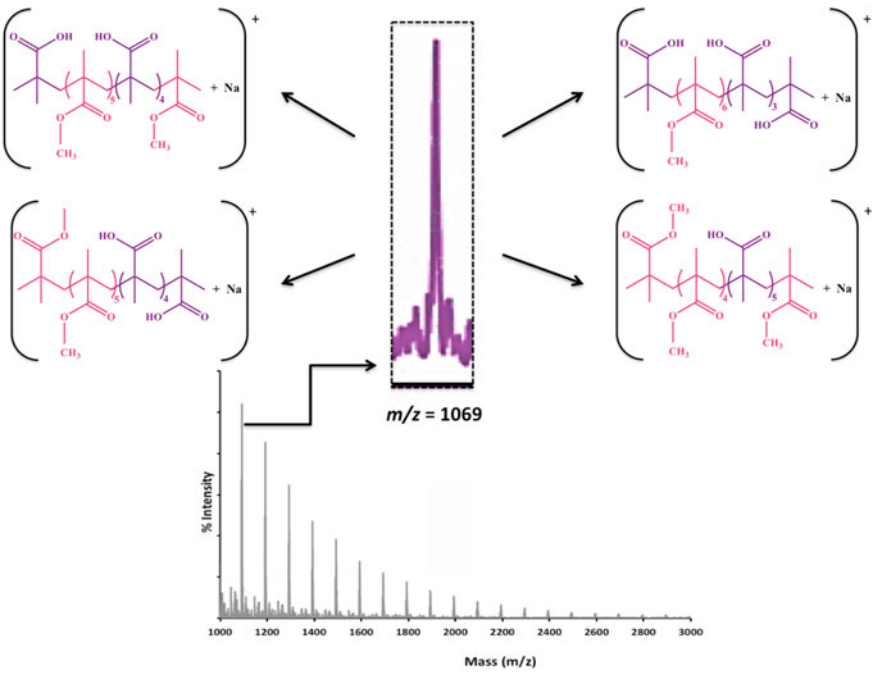

Fig. 2.9 Four structures with different end-groups proposed for the peak at *m/z* = 1069 in P(MMA-co-MAA) (5:5) MALDI spectrum (reproduces with the permission from Hosseini et al. [20])

2.5 Role of MALDI Analysis in Bio-sensing Application of P(MMA-Co-MAA)

2.5.1 Reaction's Parameters

PMMA is the well-established material of choice for fabrication of analytical platforms due to its unique properties [4]. Nevertheless, this highly commercial polymer is inert in its nature. In the other words, PMMA lacks the presence of active functionalities in its structure thus it does not promote analyte-surface interaction.

In this study, we have synthesized a new type of copolymer in different compositions that can be suitable substitutions for fabrication of ELISA well plates instead of existing PMMA materials. Newly developed copolymer compositions possess almost all of the characteristics of the commercial PMMA. The minor difference is the presence of MAA monomers in synthesis procedure. This monomer, contains one of the desirable functional groups (–COOH), which is known as a relatively active functional groups in interacting with proteins [17, 19, 23]. Existence of –COOH groups can significantly promote protein immobilization not

only via physical attachment but also through strong way of chemical immobilization. In the other words, chance of successful protein immobilization on a surface with available –COOH groups is higher as such functionalities can be used for protein attachment via carbodiimide chemistry or even through amine-bearing spacers [19, 35].

However, if one aspect matters more than the presence of such functional groups on the surface, it would be the proper distribution of such functionalities on the bioreceptor surface [10, 17–19, 23–25]. As it was explained in Sect. 2.2, different –COOH distribution on the surface could be obtained by variation of the molar ratios of the monomers (MMA/MAA). By controlling the number of the monomers involved in polymerization reaction, the optimal distribution of –COOH groups in the designed platform can be achieved.

If designed material contains too many of the functional groups on the surface, it may result in an inefficient surface immobilization due to the steric repulsion [18, 19, 23, 36]. As Fig. 2.10 depicts, an overly crowded surface with functionalities does not necessarily result in an efficient antibody immobilization as neighboring immobilized antibodies prevent approaching ones to accommodate themselves on the engineered surface functional groups.

On the other hand, if the platform contains insufficient number of –COOH groups for protein attachment, it may cause the approaching proteins to "fall" on the surface instead of a proper attachment to the available –COOH groups (Fig. 2.11). It is known that proteins are sensitive biomolecular entities towards the solid phases thus they might lose their activity in close proximity of the surface. Therefore, it can be concluded that the optimal presence of available functional groups is essential for successful biomolecular attachment and subsequent virus detection. Only by careful control over initial molar ratios of the monomer an optimal platform with desirable concentration of functional groups can be

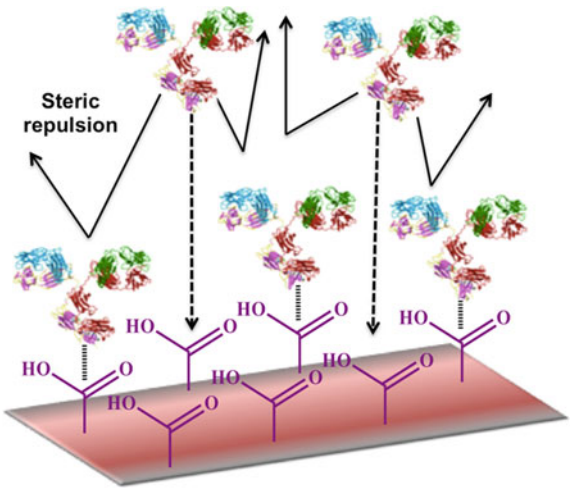

Fig. 2.10 Unsuccessful immobilization of the analyte on the surface due to the steric hindrance caused by neighboring immobilized analytes

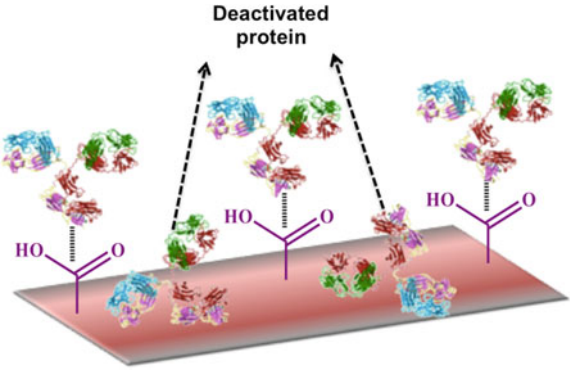

Fig. 2.11 Unsuccessful immobilization of the analyte on the surface due to the insufficient number of functional groups on the surface that led to the deactivation of the proteins due to the close proximity of the analytes to the surface

produced. In that path, MALDI analysis is of a great assistance as this technique gives an overall confirmation on the participation of the pre-determined monomers in formation of the polymer chains. Finding optimal distribution of the functional groups on the surface, however, can only be assessed by direct performance evaluation of the material in the actual analytical assay.

2.5.2 Chemistry Aspect

Understanding the major forces that play the key important roles in biomolecular interaction is essential when the analyte-surface interaction is concerned. Figure 2.12 outlines some of these main forces that have a great impact on biomolecular interactions. Among different important forces involved in analyte-surface interaction, three main forces have the vital influence in physical immobilization of the proteins. These forces are namely: ionic attraction, hydrophobic interaction and hydrogen bonding [37]. It is believed that among these forces, H-bonding offers the most strong protein attachment to the surface. As Fig. 2.12 depicts, presence of –COOH and $–COOCH_3$ functional groups on the surface of P(MMA-co-MAA) biochips imposes all the major forces in protein immobilization. Available –COOH groups of the biochips form the strong H-bonds with $–NH_2$ groups of the proteins, while both mentioned functionalities ($–NH_2$ and –COOH) in their amphoteric form might result in an electrostatic interaction (ionic attraction). Therefore, it can be concluded that by introducing sufficient number of –COOH groups to the structure of the copolymer, the chance of stronger protein attachment via dominant H-bonding increases [35]. It can be clearly understood that the minor alteration in the structure of the material from PMMA to P(MMA-co-MAA) can lead to the major improvement in the performance of the bioreceptor platform.

Available $–COOCH_3$ groups on the surface, however, are the promoters of hydrophobic interaction. The hydrophobic nature of this functionality attracts the

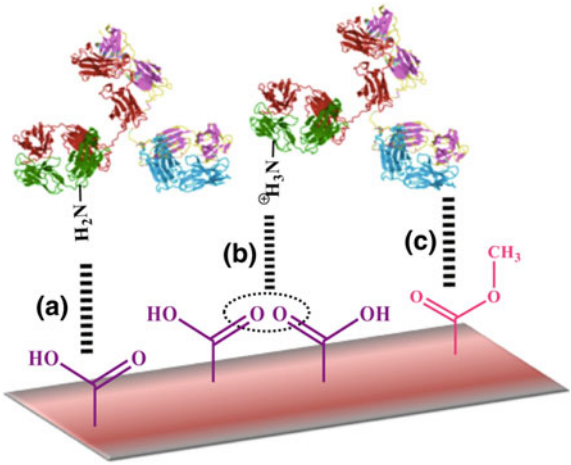

Fig. 2.12 Different possible interactions between surface functionalities of P(MMA-co-MAA) biochips and biomolecular entities such as antibodies: hydrogen bonding (**a**); ionic attraction (**b**) and hydrophobic interaction (**c**)

proteins towards the surface. Nonetheless, as it was mentioned before, this is the secondary force after strong H-bonding that can be offered by –COOH groups derived from MAA segments. In that perspective, the detailed characteristics of the developed bioreceptor can be closely tuned by tuning the concentration of functional groups at the interface with biomolecules. To achieve such a careful control over the engineered surface, MALDI analysis plays a vital role in understanding of the exact molecular structure of the copolymers.

2.5.3 Physical Aspect

While chemical properties of the developed material for bio-sensing application is highly important, physical characteristics of the developed platforms plays a major role as well. As it was explained, additional monomer of MAA changes the structure of the polymeric material (PMMA) to a copolymer structure described as P(MMA-co-MAA). This additional monomer (MAA) introduces the presence of –COOH functional groups into the structure of the copolymer compositions. Available –COOH groups of P(MMA-co-MAA) are hydrophilic in their nature thus imposing the same quality to the synthesized copolymer as well. As the molar ratio of the MAA in polymerization reaction increases, the number of –COOH groups increases, which subsequently would increase the general hydrophilicity of the compound as well. Hydrophilic materials are softer in their physical appearance. By increasing the molar ratio of the MAA segments, resultant copolymer with higher concentrations of the MAA was found to be softer. In particular, P(MMA-co-MAA) (5:5) was formed as a gel-like material instead of a hard plastic. This specific composition has obviously failed in fulfilling the basic requirement of a suitable plastic material for fabrication of the analytical platforms such as ELISA well plate.

This fact, to a considerable extent, proves the necessity of the careful control over reaction parameters, which eventually have a significant effect on the physical properties of the final product. In that path, MALDI analysis along with other useful analytical techniques provides a better understanding of the engineered macromolecule designed for bio-sensing applications.

References

1. Li X, Zhang B, Li W, Lei X, Fan X, Tian L, Zhang H, Zhang Q. Preparation and characterization of bovine serum albumin surface-imprinted thermosensitive magnetic polymer microsphere and its application for protein recognition. Biosens Bioelectr 2014;51:261–267.
2. Nie X-M, Huang R, Dong C-X, Tang L-J, Gui R, Jiang J-H. Plasmonic ELISA for the ultrasensitive detection of Treponema pallidum. Biosens Bioelectron. 2014;58:314–9.
3. Lin T-W, Kekuda D, Chu C-W. Label-free detection of DNA using novel organic-based electrolyte-insulator-semiconductor. Biosens Bioelectron. 2010;25:2706–10.
4. Hosseini S, Ibrahim F. Current optical biosensors in clinical practice. In: Novel polymeric biochips for enhanced detection of infectious diseases. Berlin: Springer; 2016. p. 1–12.
5. Kirsch J, Siltanen C, Zhou Q, Revzin A, Simonian A. Biosensor technology: recent advances in threat agent detection and medicine. Chem Soc Rev. 2013;42:8733–68.
6. Le Goff A, Holzinger M, Cosnier S. Enzymatic biosensors based on SWCNT-conducting polymer electrodes. Analyst. 2011;136:1279–87.
7. Liu Y, Li CM. Advanced immobilization and amplification for high performance protein chips. Anal Lett. 2012;45:130–55.
8. Turner APF. Biosensors: sense and sensibility. Chem Soc Rev. 2013;42:3184–96.
9. Alcon S, Talarmin A, Debruyne M, Falconar A, Deubel V, Flamand M. Enzyme-linked immunosorbent assay specific to dengue virus type 1 nonstructural protein NS1 reveals circulation of the antigen in the blood during the acute phase of disease in patients experiencing primary or secondary infections. J Clin Microbiol. 2002;40:376–81.
10. Hosseini S, Ibrahim F, Djordjevic I, Koole LH. Recent advances in surface functionalization techniques on polymethacrylate materials for optical biosensor applications. Analyst. 2014;139:2933–43.
11. Dähnrich C, Pares A, Caballeria L, et al. New ELISA for detecting primary biliary cirrhosis-specific antimitochondrial antibodies. Clin Chem. 2009;55:978–85.
12. Xu H, Di B, Y-x Pan, et al. Serotype 1-specific monoclonal antibody-based antigen capture immunoassay for detection of circulating nonstructural protein NS1: implications for early diagnosis and serotyping of dengue virus infections. J Clin Microbiol. 2006;44:2872–8.
13. Lu W, Cao X, Tao L, Ge J, Dong J, Qian W. A novel label-free amperometric immunosensor for carcinoembryonic antigen based on Ag nanoparticle decorated infinite coordination polymer fibres. Biosens Bioelectron. 2014;57:219–25.
14. Hong C-C, Chen C-P, Horng J-C, Chen S-Y. Point-of-care protein sensing platform based on immuno-like membrane with molecularly-aligned nanocavities. Biosens Bioelectron. 2013;50:425–30.
15. Chen J-P, Ho K-H, Chiang Y-P, Wu K-W. Fabrication of electrospun poly(methyl methacrylate) nanofibrous membranes by statistical approach for application in enzyme immobilization. J Membr Sci. 2009;340:9–15.
16. Tang C, Saquing CD, Sarin PK, Kelly RM, Khan SA. Nanofibrous membranes for single-step immobilization of hyperthermophilic enzymes. J Membr Sci. 2014;472:251–60.

17. Hosseini S, Ibrahim F, Djordjevic I, et al. Synthesis and characterization of methacrylic microspheres for biomolecular recognition: ultrasensitive biosensor for dengue virus detection. Eur Polymer J. 2014;60:14–21.
18. Hosseini S, Ibrahim F, Djordjevic I, Koole LH. Polymethyl methacrylate-co-methacrylic acid coatings with controllable concentration of surface carboxyl groups: A novel approach in fabrication of polymeric platforms for potential bio-diagnostic devices. Appl Surf Sci. 2014;300:43–50.
19. Hosseini S, Ibrahim F, Djordjevic I, et al. Synthesis and processing of ELISA polymer substitute: the influence of surface chemistry and morphology on detection sensitivity. Appl Surf Sci. 2014;317:630–8.
20. Hosseini S, Ibrahim F, Djordjevic I, Aeinehvand MM, Koole LH. Structural and end-group analysis of synthetic acrylate co-polymers by matrix-assisted laser desorption time-of-flight mass spectrometry: distribution of pendant carboxyl groups. Polymer Testing 2014;40:273–279. doi:10.1016/j.polymertesting.2014.09.017.
21. Mitchell JS. Spin-coated methacrylic acid copolymer thin films for covalent immobilization of small molecules on surface plasmon resonance substrates. Eur Polymer J. 2011;47:16–23.
22. Grama S, Boiko N, Bilyy R, et al. Novel fluorescent poly(glycidyl methacrylate) – Silica microspheres. Eur Polymer J. 2014;56:92–104.
23. Hosseini S, Ibrahim F, Rothan HA, et al. Aging effect and antibody immobilization on –COOH exposed surfaces designed for dengue virus detection. Biochem Eng J. 2015;99: 183–92.
24. Hosseini S, Aeinehvand MM, Uddin SM, et al. Microsphere integrated microfluidic disk: synergy of two techniques for rapid and ultrasensitive dengue detection. Scientific reports 2015. p. 5.
25. Hosseini S, Azari P, Farahmand E, et al. Polymethacrylate coated electrospun PHB fibers: An exquisite outlook for fabrication of paper-based biosensors. Biosens Bioelectron. 2015;69:257–64.
26. Hosseini S, Ibrahim F. An alternative chemical approach for development of polymeric analytical platforms. In: Novel polymeric biochips for enhanced detection of infectious diseases. Berlin: Springer; 2016. p. 13–21.
27. Hosseini S, Ibrahim F. Biochips fabrication and surface characterization. In: Novel polymeric biochips for enhanced detection of infectious diseases. Berlin: Springer; 2016. p. 23–37.
28. Meier MA, Schubert US. Evaluation of a new multiple-layer spotting technique for matrix-assisted laser desorption/ionization time-of-flight mass spectrometry of synthetic polymers. Rapid Commun Mass Spectrom. 2003;17:713–6.
29. Caprioli RM, Farmer TB, Gile J. Molecular imaging of biological samples: localization of peptides and proteins using MALDI-TOF MS. Anal Chem. 1997;69:4751–60.
30. Nielen MWF. MALDI time-of-flight mass spectrometry of synthetic polymers. Mass Spectrom Rev. 1999;18:309–44.
31. Adamus G, Rizzarelli P, Montaudo MS, Kowalczuk M, Montaudo G. Matrix-assisted laser desorption/ionization time-of-flight mass spectrometry with size-exclusion chromatographic fractionation for structural characterization of synthetic aliphatic copolyesters. Rapid Commun Mass Spectrom. 2006;20:804–14.
32. Carroccio S, Rizzarelli P, Puglisi C. Matrix-assisted laser desorption/ionisation time-of-flight characterisation of biodegradable aliphatic copolyesters. Rapid Commun Mass Spectrom. 2000;14:1513–22.
33. Tatro SR, Baker GR, Bisht K, Harmon JP. A MALDI, TGA, TG/MS, and DEA study of the irradiation effects on PMMA. Polymer. 2003;44:167–76.
34. Girod M, Antoine R, Lemoine J, Dugourd P, Charles L. Structural characterization of a poly (methacrylic acid)/poly (methylmethacrylate) copolymer by activated electron photo-detachment dissociation. Int J Mass Spectrom. 2013;333:27–33.

35. Hosseini S, Ibrahim F. Application of biochips in dengue virus detection. In: Novel polymeric biochips for enhanced detection of infectious diseases. Berlin: Springer; 2016, p. 39–47.
36. Goddard JM, Hotchkiss JH. Polymer surface modification for the attachment of bioactive compounds. Prog Polym Sci. 2007;32:698–725.
37. Yoon J-Y, Park H-Y, Kim J-H, Kim W-S. Adsorption of BSA on highly carboxylated microspheres—quantitative effects of surface functional groups and interaction forces. J Colloid Interface Sci. 1996;177:613–20.

http://www.springer.com/978-981-10-2355-2

Fundamentals of MALDI-ToF-MS Analysis
Applications in Bio-diagnosis, Tissue Engineering and Drug Delivery

Hosseini, S.; Martinez-Chapa, S.O.

2017, XI, 68 p. 34 illus., 31 illus. in color., Softcover
ISBN: 978-981-10-2355-2